EFFECT OF CO-DOPING DIFFERENT RARE EARTH IONS ON $CaB_6O_{10}:Sm^{3+}$, RE^{3+} (RE = Dy, Er, Gd, La, Nd, Tb) PHOSPHORS[**]

Esra Yildiz [1], Ertuğrul Erdoğmuş [2*]

[1] Yozgat Bozok University, Hemp Research Institute, Department of Basic Sciences and Health, Yozgat, Turkey
[2] Bartın University, Faculty of Engineering, Architecture and Design, Department of Environmental Engineering, Turkey; e-mail: eerdogmus@bartin.edu.tr

Sm^{3+} doped and RE^{3+} (RE = Dy, Er, Gd, La, Nd, Tb) co-doped CaB_6O_{10} phosphors were prepared at 800°C by the solid-state reaction method. The obtained powders were structurally characterized by X-ray diffraction and Fourier transform infrared analyses. The influences of co-doping rare earth ions on their luminescent properties were also investigated. The emission spectra of the $CaB_6O_{10}:Sm^{3+}$ phosphors consisted of some sharp emission peaks of Sm^{3+} ions centered at 561, 601, 649, and 708 nm, generating bright orange-red light. The concentration quenching occurred when x equals 0.05 for $CaB_6O_{10}:xSm^{3+}$ phosphor. No remarkable differences were found from excitation spectra of co-doped phosphors $CaB_6O_{10}:Sm^{3+}$, RE^{3+} in contrast with that of phosphor $CaB_6O_{10}:Sm^{3+}$. The introduction of charge compensator RE^{3+} (RE = Dy, Er, Gd, La, Nd, Tb) into the host reduced the luminescence intensity of the $CaB_6O_{10}:Sm^{3+}$ phosphors.

Keywords: *photoluminescence, rare-earth ions, CaB_6O_{10}.*

ВЛИЯНИЕ СОВМЕСТНОГО ЛЕГИРОВАНИЯ ИОНАМИ РАЗЛИЧНЫХ РЕДКОЗЕМЕЛЬНЫХ ЭЛЕМЕНТОВ НА СВОЙСТВА ЛЮМИНОФОРОВ $CaB_6O_{10}:Sm^{3+}$, RE^{3+} (RE = Dy, Er, Gd, La, Nd, Tb)

E. Yildiz [1], E. Erdoğmuş [2*]

УДК 535.37

[1] Университет Йозгат Бозок, Йозгат, Турция
[2] Бартынский университет, Бартын, Турция; e-mail: eerdogmus@bartin.edu.tr

(Поступила 21 декабря 2021, в окончательной редакции — 8 ноября 2022)

Совместно легированные ионами Sm^{3+} и RE^{3+} (RE = Dy, Er, Gd, La, Nd, Tb) люминофоры CaB_6O_{10} получены при 800°C методом твердофазной реакции. Полученные порошки структурно охарактеризованы методами рентгеноструктурного анализа и ИК-Фурье-спектроскопии. Спектры излучения люминофоров $CaB_6O_{10}:Sm^{3+}$ состояли из нескольких пиков излучения ионов Sm^{3+} с центрами 561, 601, 649, 708 нм, генерирующих яркий оранжево-красный свет. Концентрационное тушение происходило при x = 0.05 для люминофора $CaB_6O_{10}:xSm^{3+}$. Отличий спектров возбуждения легированных люминофоров $CaB_6O_{10}:Sm^{3+}$, RE^{3+} от спектров возбуждения люминофора $CaB_6O_{10}:Sm^{3+}$ не обнаружено. Введение в матрицу компенсатора заряда RE^{3+} (RE = Dy, Er, Gd, La, Nd, Tb) снижает интенсивность люминесценции люминофоров $CaB_6O_{10}:Sm^{3+}$.

Ключевые слова: *фотолюминесценция, редкоземельные ионы, CaB_6O_{10}.*

[**] Full text is published in JAS V. 90, No. 3 (http://springer.com/journal/10812) and in electronic version of ZhPS V. 90, No. 3 (http://www.elibrary.ru/title_about.asp?id=7318; sales@elibrary.ru).

Introduction. Luminescent materials containing rare-earth ions have become popular in the development of optical materials [1–4]. Commercial powder phosphors are usually based on the host matrices of tungstates [5], phosphates [6], borates [7], silicates [8], and aluminates [9], etc. Among them, borates have gained attention from many scientists as they show excellent optical properties due to their high chemical and thermal stabilization, facile synthesis, low synthetic temperature, better stability and require cost-effective raw material such as H_3BO_3 for the preparation stage [10–14]. A large band gap and covalent bond energy make alkaline earth borates potential host materials as they can be doped with rare earth elements to prepare light-emitting materials or phosphors. Borates doped with rare earth elements show remarkable luminescent properties, mainly due to the presence of abundant 4f energy levels and the transition of 4*f* electrons between different energy levels of rare-earth ions [15]. The unique electronic configuration of the 4*f* energy levels, leading to 4*f*–4*f* or 5*d*–4*f* transitions in rare earth ions, plays an important role in modern displays and lighting due to their rich emission colors [16–21]. A vast number of studies on RE ion properties in the past decades have led to extensive applications of RE ions in LEDs, displays, sensors, lasers, optical fibre amplifiers, solar control devices, etc. [22–24].

Sm^{3+} is a convenient modeling ion to study the cross-relaxation processes and spatial distribution of the activator in host-matrix [25]. In this paper, we successfully synthesized Sm^{3+} doped and RE^{3+} (RE = Dy, Er, Gd, La, Nd, Tb) co-doped CaB_6O_{10} phosphors via the solid-state reaction method. The luminescence properties of CaB_6O_{10}:Sm^{3+} phosphors were investigated by modifying co-doped Dy^{3+}, Er^{3+}, Gd^{3+}, La^{3+}, Nd^{3+}, and Tb^{3+} ions in the host.

Experiment. Undoped, Sm^{3+} doped and RE^{3+} (RE = Dy, Er, Gd, La, Nd, Tb) co-doped CaB_6O_{10} phosphors were prepared by a solid-state reaction method. The starting materials were $CaCO_3$, H_3BO_3, Sm_2O_3, Dy_2O_3, Er_2O_3, Gd_2O_3, La_2O_3, Nd_2O_3 and Tb_2O_3 of high-purity analytical reagent grade chemicals. The chemical compositions are $Ca_{1-x}Sm_xB_6O_{10}$ (x = 0.01,0.02, 0.03, 0.04, 0.05, 0.06), $Ca_{0.90}Sm_{0.05}Dy_{0.05}B_6O_{10}$, $Ca_{0.90}Sm_{0.05}Er_{0.05}B_6O_{10}$, $Ca_{0.90}Sm_{0.05}Gd_{0.05}B_6O_{10}$, $Ca_{0.90}Sm_{0.05}La_{0.05}B_6O_{10}$, $Ca_{0.90}Sm_{0.05}Nd_{0.05}B_6O_{10}$, and $Ca_{0.90}Sm_{0.05}Tb_{0.05}B_6O_{10}$. Stoichiometric amounts of the starting materials were thoroughly mixed in an agate mortar and homogeneously mixed and placed in an alumina crucible at room temperature. First, the mixtures were heated up to 400ºC and kept at this temperature for 1 h in the air, after which, grinding and homogenization of pre-annealed mixtures were performed. Afterwards, the pre-annealed mixtures were sintered at 800ºC for 5 h in the air, in an alumina crucible.

X-ray powder diffraction (XRD) patterns of the synthesized phosphors were obtained using a Bruker AXS D8 Advance diffractometer with CuK_α radiation, 30 kV, 15 mA, and λ = 1.54051 Å. The Fourier transform infrared spectra between 500 and 1500 cm^{-1} were measured with a Shimadzu 8303 FTIR spectrometer. The PL emission and excitation spectra of powder phosphors were measured by using a Thermo Scientific Lumina fluorescence spectrophotometer with a 150 W xenon lamp as the excitation source. All measurements were carried out at room temperature.

Results and discussion. *Structural characterization.* The XRD patterns of CaB_6O_{10}:Sm^{3+} and CaB_6O_{10}:Sm^{3+}, RE^{3+} (RE = Dy, Er, Gd, La, Nd, Tb) phosphors are presented in Fig. 1. As indicated by the figure, the XRD patterns are in agreement with JCPDS (01-076-8428) and the XRD data of CaB_6O_{10} in [26]. All phosphors crystallize in the monoclinic system with a space group of $P2_1/c$ and lattice parameters of a = 9.799 Å, b = 8.705 Å, c = 9.067 Å, and Z = 4. The XRD patterns of phosphors matched well with the standard reflections of host CaB_6O_{10} for all dopant ions. No peaks of the used raw materials or other allotropic forms were detected. The absence of any secondary phase indicates that the samples crystallized in the lattice structure are similar to that of the host, and the dopant ions were successfully dissolved into the host lattice.

To further confirm the coordination environment of B–O in the $Sr_2B_2O_5$ structure, the IR spectra of $Sr_2B_2O_5$ was measured at room temperature (Fig. 2). The IR absorption at wave numbers smaller than 450 cm^{-1} mainly originates from the lattice dynamic modes. The $Sr_2B_2O_5$ material from the analysis of the spectrum IR, BO_3^{3-} ion has been identified as two triangular BO_3 groups at one corner sharing an O atom. For an isolated, triangular BO_3 group, the vibrations are in the region of ν_3 = 1100–1400 cm^{-1} (asymmetric stretch of B–O), ν_1 = 900–1000 cm^{-1} (symmetric stretch of B–O), ν_2 = 700–900 cm^{-1} (out-of-plane bend), and ν_4 = 450–650 cm^{-1} (in-plane bend) [27, 28].

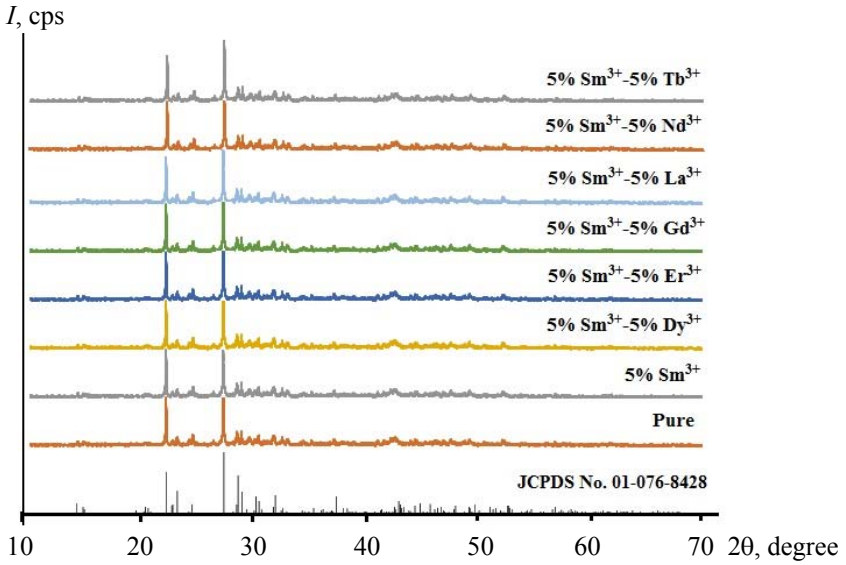

Fig. 1. XRD patterns of CaB_6O_{10}, $CaB_6O_{10}:Sm^{3+}$, $CaB_6O_{10}:Sm^{3+}$, Dy^{3+}, $CaB_6O_{10}:Sm^{3+}$, Er^{3+}, $CaB_6O_{10}:Sm^{3+}$, Gd^{3+}, $CaB_6O_{10}:Sm^{3+}$, La^{3+}, $CaB_6O_{10}:Sm^{3+}$, Nd^{3+}, $CaB_6O_{10}:Sm^{3+}$, Tb^3 phosphors and the standard data JCPDS card No. 01-076-8428 of CaB_6O_{10} compound.

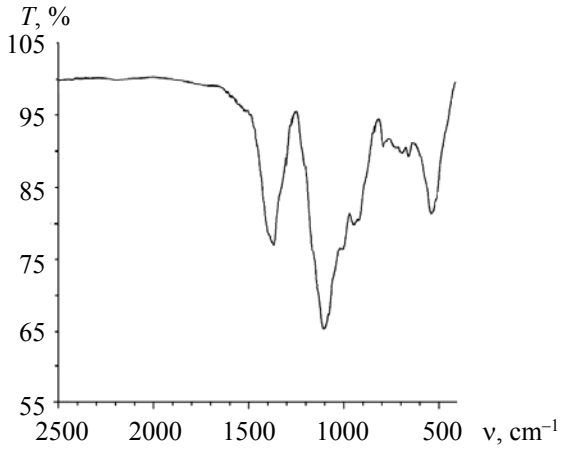

Fig. 2. The infrared spectrum of the CaB_6O_{10} at room temperature.

Photoluminescence properties. $CaB_6O_{10}:Sm^{3+}$ phosphor. The PL excitation spectrum of 5% Sm-doped CaB_6O_{10} powder phosphor for emission at 601 nm wavelength, in 350–450 nm with five peaks, located at 357, 367, 397, and 433 nm, is shown in Fig. 3a. Nearly no PL properties can be obtained from the undoped sample. There are certain excitation bands that are attributed to the 4*f*–4*f* intra-configurational transitions of Sm^{3+} ions in the phosphors. All transitions in the absorption spectrum of Sm^{3+} start from the ground state $^6H_{5/2}$ to the various excited states in the PL excitation spectrum. These excitation peaks are located at 357 nm ($^6H_{5/2}\rightarrow{}^6H_{13/2}$), 367 nm ($^6H_{5/2}\rightarrow{}^4D_{3/2}$), 392 nm ($^6H_{5/2}\rightarrow{}^6P_{7/2}$), 397 nm ($^6H_{5/2}\rightarrow{}^4F_{7/2}$), and 433 nm ($^6H_{5/2}\rightarrow{}^4G_{9/2}$) [29–31]. From the excitation spectrum, it was found that, compared to the other transitions, the intensity of the *f–f* transition at 397 nm is high and has been chosen for the measurement of the emission spectrum of CaB_6O_{10}:5%Sm^{3+} phosphors. The most intense peak at 397 nm clearly indicates that this phosphor can be effectively excited by near-UV LED chips (350–420 nm), which is certainly needed for potential applications in w-LEDs.

The emission spectrum of 5% Sm-doped CaB_6O_{10} is given in Fig. 3b, which was measured in the 450–750 nm range. The emission spectrum of CaB_6O_{10}:5%Sm^{3+} phosphors exhibited four emission peaks corresponding to $^4G_{5/2}\rightarrow{}^6H_{5/2}$ (561 nm), $^4G_{5/2}\rightarrow{}^6H_{7/2}$ (601 nm), $^4G_{5/2}\rightarrow{}^6H_{9/2}$ (649 nm) and $^4G_{5/2}\rightarrow{}^6H_{11/2}$ (708 nm) transition of Sm^{3+} [32–34]. Among them, transition $^4G_{5/2}\rightarrow{}^6H_{7/2}$ (601 nm) has a relatively higher

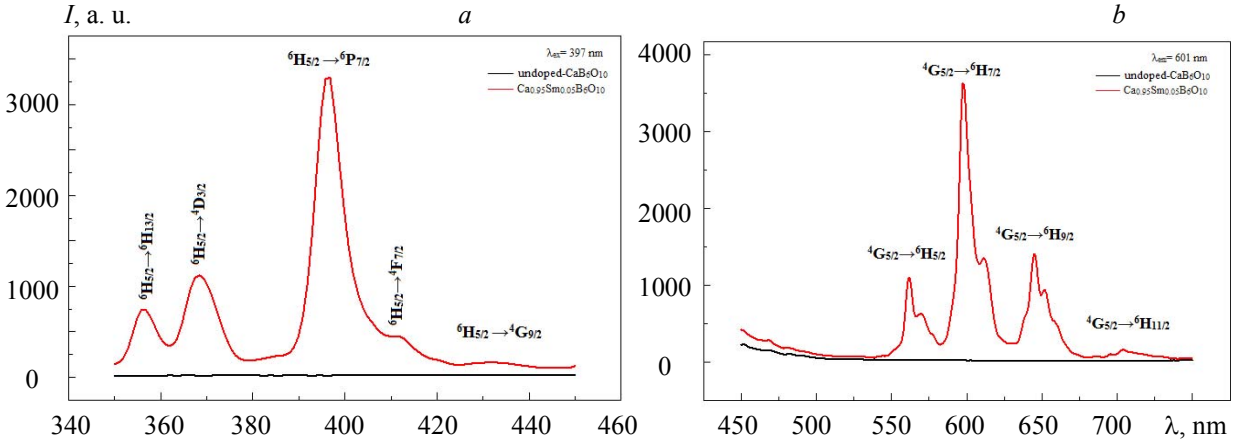

Fig. 3. Excitation (a) and emission (b) spectra of undoped-CaB_6O_{10} and $Ca_{0.95}Sm_{0.05}B_6O_{10}$ at room temperature.

emission intensity than the other transitions. The first one at 561 nm ($^4G_{5/2}\rightarrow{}^6H_{5/2}$) is a magnetic-dipole transition, the second at 601 nm ($^4G_{5/2}\rightarrow{}^6H_{7/2}$) is a partly magnetic and partly a forced electric-dipole transition, and the other at 649 nm ($^4G_{5/2}\rightarrow{}^6H_{9/2}$) is a purely electric dipole transition which is sensitive to the crystal field. The intensity ratio of the electric-dipole to magnetic-dipole transition can be used to measure the symmetry of the local environment of the trivalent 4*f* ions. In general, the electric-dipole transition will be of greater intensity for a more asymmetric local environment. In the present investigation, differences were not observed in the intensities of electric-dipole ($^4G_{5/2}\rightarrow{}^6H_{9/2}$) and magnetic-dipole ($^4G_{5/2}\rightarrow{}^6H_{5/2}$) transitions. Furthermore, emission bands split into components, whereby the splitting of energy levels may have been caused by the crystal field interaction.

The PL spectra of CaB_6O_{10}:$x$$Sm^{3+}$ phosphors with different doping concentrations (x = 0.01, 0.02, 0.03, 0.04, 0.05, and 0.06) of Sm^{3+} are presented in Fig. 3b. It is also found in Fig. 4 that, except for the emission intensities, the PL spectra have similar profiles. The inset of in Fig. 4 (in fig.4 no insert!!!) shows the function of emission intensity on the concentration of Sm^{3+} excited at 397 nm, respectively. The emission intensity firstly increases with the increasing Sm^{3+} concentration, reaching a maximum when the concentration is 5 mol.%. The concentration-quenching phenomenon occurs during excitation, thus the luminous intensity decreases, and therefore, the optimum mol fraction for achieving the highest luminous intensity of Sm^{3+} in CaB_6O_{10} matrix is 0.05. The energy loss at the emission level initiated by the cross-relaxation between the excited ions might be the main cause of the concentration quenching. The fluorescent emission of Sm^{3+} was mainly due to the transitions from a metastable level $^4G_{5/2}$ to level ^6H_J. The quenching of luminescence from the $^4G_{5/2}$ state is also due to a cross-relaxation process between the excited Sm^{3+} ions and unexcited Sm^{3+} ions nearby. Since the energy gap between the $^4G_{5/2}$ emission level and the lower-lying $^6F_{11/2}$ level is about 7200 cm^{-1}, the possibility of multi-phonon relaxation in Sm^{3+} is negligible. Taking into account the energy levels of Sm^{3+} in CaB_6O_{10} phosphors, the luminescence level may be depopulated mainly via the resonant cross-relaxation paths including ($^4G_{5/2}\rightarrow{}^6F_{11/2}$)–($^6H_{5/2}\rightarrow{}^6F_{5/2}$) and ($^4G_{5/2}\rightarrow{}^6F_{5/2}$)–($^6H_{5/2}\rightarrow{}^6F_{11/2}$) [35]. A considerable amount of excited ions on the $^4G_{5/2}$ level were transferred from the $^4G_{5/2}$ level to the $^6F_{9/2}$ level due to the cross-relaxation process; therefore, several useful excited ions were consumed through the radiation and relaxation processes and the fluorescence emission was thereby reduced.

CaB_6O_{10}:Sm^{3+}, RE^{3+} (RE = Dy, Er, Gd, La, Nd, Tb) phosphor. In order to research the interaction between Sm^{3+} and Dy^{3+}, Er^{3+}, Gd^{3+}, La^{3+}, Nd^{3+} and Tb^{3+}, co-doped CaB_6O_{10} phosphors were prepared and their luminescence properties were studied.

We chose 5 mol.% Sm^{3+} and 5 mol.% Dy^{3+}, Er^{3+}, Gd^{3+}, La^{3+}, Nd^{3+} and Tb^{3+} co-doped host as an example to discuss their luminescence properties. The excitation and emission spectra of the $Ca_{0.90}Sm_{0.05}Dy_{0.05}B_6O_{10}$, $Ca_{0.90}Sm_{0.05}Er_{0.05}B_6O_{10}$, $Ca_{0.90}Sm_{0.05}Gd_{0.05}B_6O_{10}$, $Ca_{0.90}Sm_{0.05}La_{0.05}B_6O_{10}$, $Ca_{0.90}Sm_{0.05}Nd_{0.05}B_6O_{10}$, and $Ca_{0.90}Sm_{0.05}Tb_{0.05}B_6O_{10}$ phosphors are shown in Fig. 5. The excitation and emission bands are due to the transitions of Sm^{3+} ions as seen in Fig. 3b. The electronic transitions of Dy^{3+}, Er^{3+}, Gd^{3+}, La^{3+}, Nd^{3+} and Tb^{3+} ions were not observed and RE^{3+} co-doped CaB_6O_{10}:Sm^{3+} decreased the emission intensity.

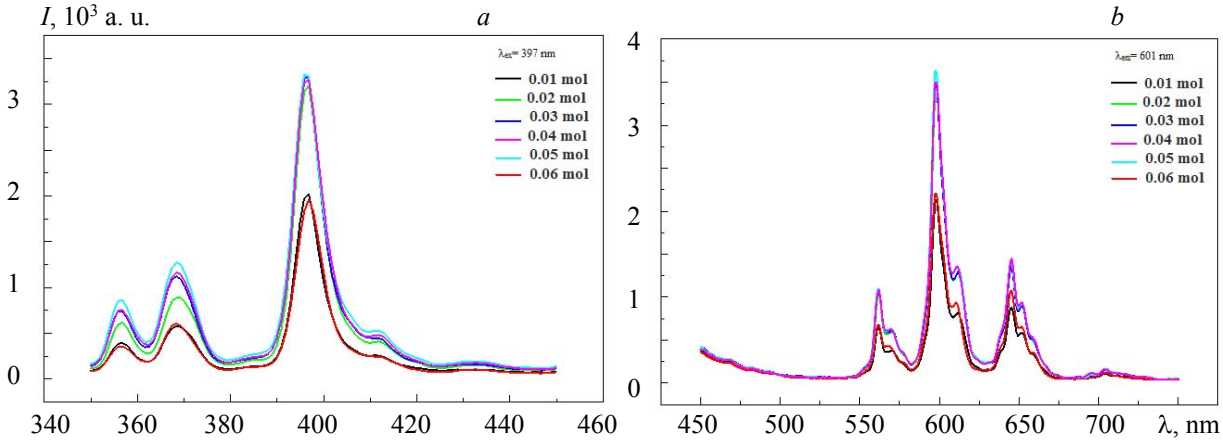

Fig. 4. Excitation (a) and emission (b) spectra of CaB_6O_{10}:$x$$Sm^{3+}$ phosphors (x = 0.01, 0.02, 0.03, 0.04, 0.05, and 0.06).

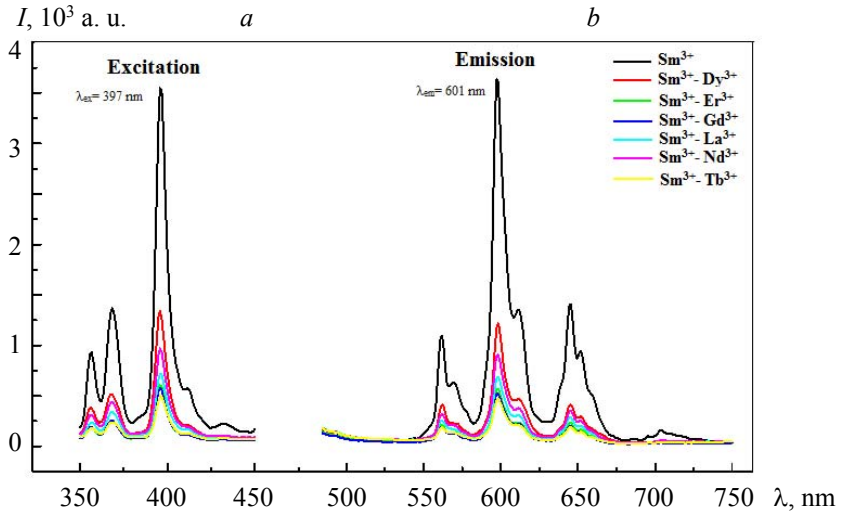

Fig. 5. Excitation (a) and emission spectra (b) $Ca_{0.90}Sm_{0.05}Dy_{0.05}B_6O_{10}$, $Ca_{0.90}Sm_{0.05}Er_{0.05}B_6O_{10}$, $Ca_{0.90}Sm_{0.05}Gd_{0.05}B_6O_{10}$, $Ca_{0.90}Sm_{0.05}La_{0.05}B_6O_{10}$, $Ca_{0.90}Sm_{0.05}Nd_{0.05}B_6O_{10}$, and $Ca_{0.90}Sm_{0.05}Tb_{0.05}B_6O_{10}$ phosphors.

In many inorganic materials, excessive doping of emission ions usually decreases the emission intensity remarkably. The phenomenon is called quenching, which is caused by the migration of excitation energy between the emission ions or energy migration to quenching centers where the excitation energy is lost by non-radiative transition. The emission intensity related to Sm^{3+} ions was reduced dramatically after the optimization of the Dy^{3+}, Er^{3+}, Gd^{3+}, La^{3+}, Nd^{3+} and Tb^{3+} ion concentration of 5 mol.%, due to a concentration quenching effect. The Dy^{3+}, Er^{3+}, Gd^{3+}, La^{3+}, Nd^{3+} and Tb^{3+} aggregates may quench the absorbed excitation energy rather than transfer it to activator ions, which results in decreased emission intensity of the activator ions.

Conclusions. Sm^{3+} single-doped and Dy^{3+}, Er^{3+}, Gd^{3+}, La^{3+}, Nd^{3+}, and Tb^{3+} co-doped CaB_6O_{10} phosphors were prepared by a solid-state reaction method. XRD results showed that the monoclinic structure CaB_6O_{10} was successfully synthesized and the introduction of Sm^{3+} and Dy^{3+}, Er^{3+}, Gd^{3+}, La^{3+}, Nd^{3+}, and Tb^{3+} did not have an apparent effect on the crystal structure of CaB_6O_{10}. The results show that the CaB_6O_{10}:Sm^{3+} phosphor can be efficiently excited by 397 nm light, emitting intense orange-red light, and its spectrum is mainly composed of four emission peaks at 561 nm ($^4G_{5/2}\rightarrow{}^6H_{5/2}$), 601 ($^4G_{5/2}\rightarrow{}^6H_{7/2}$), 649 ($^4G_{5/2}\rightarrow{}^6H_{9/2}$), and 708 nm ($^4G_{5/2}\rightarrow{}^6H_{11/2}$). The PL intensity of the CaB_6O_{10}:Sm^{3+} gradually increased with increasing Sm^{3+} doping. The PL intensity reached its maximum when the Sm^{3+} doping was 0.05. RE^{3+} (Dy, Er, Gd, La, Nd, Tb) co-doped CaB_6O_{10}:Sm^{3+} phosphor decreased the emission intensity, whereas the electronic transitions of RE^{3+} ions were not observed. The results indicate that this kind of CaB_6O_{10}:Sm^{3+} phosphor would be promising as an orange-red emitting phosphor for white light-emitting diodes.

REFERENCES

1. Y. Wang, Y. H. Wang, *J. Alloys Compd*., **425**, L5–L7 (2016).
2. Y. H. Wang, C. F. Wu, J. C. Zhang, *Mater. Res. Bull*., **41**, 1571–1577 (2006).
3. B. Vengala Rao, S. Buddhudu, *Mater. Chem. Phys*., **111**, 65–68 (2008).
4. Y. G Su, L. P. Li, G. S. Li, *Chem. Commun*., **34**, 4004–4006 (2008).
5. S. Neeraj, N. Kijima, A. K. Cheetham, *Chem. Phys. Lett*., **387**, 2–6 (2004).
6. N. Hashimoto, Y. Takada, K. Sato, S. Ibuki, *J. Lumin*., **48-49**, 893–897 (1991).
7. F. Shen, D. He, H. Liu, J. Xu, *J. Lumin*., **122**, 973–975 (2007).
8. E. Öztürk, E. Karacaoğlu, E. Uzun, *J. Lumin*., **204**, 51–58 (2018).
9. E. Nakazawa, Y. Murazaki, S. Saito, *J. Appl. Phys*., **100**, 113113–113120 (2006).
10. G. Chadeyron, R. Mahiou, M. El-Ghozzi, A. Arbus, D. Zambon, J. Cousseins, *J. Lumin*., **72**, 564–566 (1997).
11. L. Lou, D. Boyer, G. Bertrand-Chadeyron, E. Bernstein, R. Mahiou, J. Mugnier, *Opt. Mater*., **15**, 1–6 (2000).
12. M. Ren, J. H. Lin, Y. Dong, L. Q. Yang, M. Z. Su, L. P. You, *Chem. Mater*., **11**, 1576–1580 (1999).
13. R. C. Ropp, Luminescence and the Solid State, 2nd ed., Elsevier, The Netherlands (1991).
14. H. Zhu, Y. Li, L. Zhang, S. Suo, A. Sun, M. Lu, *Optoelectron. Adv. Mat*., **6**, 555–559 (2012).
15. O. Dincer, A. Ege, *J. Lumin*., **138**, 174–178 (2013).
16. H. H. Xiong, C. Zhu, X. Zhao, Z. Q. Wang, H. Lin, *Adv. Mater. Sci. Eng*., 2014, **2014**, 1–7 (2014).
17. E. Öztürk, E. Karacaoğlu, V. Kalem, *Luminescence*, **35**, 406–411 (2020).
18. D. T. Lien, D. T. Huong, L. V. Vu, N. N. Long, *J. Lumin*., **161**, 389–394 (2015).
19. L. Wu, B. Wang, Y. Zhang, *Dalton Trans*., **43**, 13845–13851 (2014).
20. E. Pekpak, A. Yilmaz, G. Ozbayoglu, *Open Miner. Process*., J. **3**, 14–24 (2010).
21. V. Neharika, J. Kumar, V. K. Sarma, O. M. Singh, H. C. Ntwaeaborwa, *J. Electron Spectrosc. and Related Phenom.*, **206**, 52–57 (2016).
22. H. Bouchouicha, G. Panczer, D. Ligny, *J. Lumin*., **169**, 528–533 (2014).
23. C. Zhu, Y. Yang, X. Liang, S. Yuan, G. Chen, *J. Lumin*., **126**, 707–710 (2007).
24. S. Arunkumar, K. Marimuthu. *J. Lumin*., **139**, 6–15 (2013).
25. G. E. Malashkevichab, V. N. Sigaev, N. V. Golubev, E. K. Mamadzhanova, A. A. Sukhodola, A. Palearic, P. D. Sarkisov, A. N. Shimko, *Mater. Chem. and Phys*., **137**, 48–54 (2012).
26. X. Chen, M. Li, X. Chang, H. Zang, W. Xiao, *J. Alloys Compd*., **464**, 332–336 (2008).
27. W. G. Zou, L. Meng Kai, G. Feng, *Mater. Sci. Eng. B*., **127**, 134–137 (2006).
28. G. Blasse, *Solid State Chem*., **18**, 79–171 (1988).
29. Z. Xia, D. Chen, *J. Am. Ceram. Soc*., **93**, 1397–1401 (2010).
30. G. R. Dillip, P. Mohan Kumar, B. Deva Prasad Raju, S. J. Dhoble, *J. Lumin*., **134**, 333–338 (2013).
31. V. Singh, S. Watanable, T. K. Gundu Rao, J. F. D. Chubaci, H. Young Kwak, *J. Non-Crystal. Solids*, **356**, 1185–1190 (2010).
32. G. Y. Dong, C. C. Hou, Z. P. Yang, P. F. Liu, H. Y. Dong, X. S. Liang, *J. Optoelectron. Laser*, **25**, 89–93 (2014).
33. P. Dalawai Sa, A. B. Gadkari, P. N. Vasambekar, *Rare Met*., **34**, 133–136 (2015).
34. L. Zhao, W. Yonfeng, C. Jing, Z. Yuanra, Z. Xicheng, M. Zhixin, *J. Rare Earths*., **34**, 143–147 (2016).
35. M. Sobczyk, D. Szymański, *J. Lumin*., **142**, 96–102 (2013)